Journal of Power Sources 196 (2011) 3565–3571

Contents lists available at ScienceDirect

Journal of Power Sources

journal homepage: www.elsevier.com/locate/jpowsour

A novel approach to determine the in-plane thermal conductivity of gas diffusion layers in proton exchange membrane fuel cells

E. Sadeghi [a,b,*], N. Djilali [a], M. Bahrami [b]

[a] Department of Mechanical Engineering, and Institute for Integrated Energy Systems, University of Victoria, P.O. Box 3055, Victoria, BC, V8W 3P6, Canada
[b] Mechatronic Systems Engineering, School of Engineering Science, Simon Fraser University, Surrey, BC V3T 0A3, Canada

ARTICLE INFO

Article history:
Received 20 September 2010
Received in revised form
28 November 2010
Accepted 29 November 2010
Available online 4 December 2010

Keywords:
Conduction heat transfer
In-plane thermal conductivity
Fibrous porous media
Anisotropic micro-structure
Polytetrafluoroethylene coating

ABSTRACT

Heat transfer through the gas diffusion layer (GDL) is a key process in the design and operation of a proton exchange membrane (PEM) fuel cell. The analysis of this process requires determination of the effective thermal conductivity. This transport property differs significantly in the through-plane and in-plane directions due to the anisotropic micro-structure of the GDL.

A novel test bed that allows separation of in-plane effective thermal conductivity and thermal contact resistance in GDLs is described in this paper. Measurements are performed using Toray carbon paper TGP-H-120 samples with varying polytetrafluoroethylene (PTFE) content at a mean temperature of 65–70 °C. The measurements are complemented by a compact analytical model that achieves good agreement with experimental data. The in-plane effective thermal conductivity is found to remain approximately constant, $k \approx 17.5\,\mathrm{W\,m^{-1}\,K^{-1}}$, over a wide range of PTFE content, and its value is about 12 times higher than that for through-plane conductivity.

1. Introduction

The temperature distribution in a proton exchange membrane (PEM) fuel cell is non-uniform due to the electrochemical reaction and associated irreversibilities [1–5]. Accurate knowledge of the temperature distribution and associated heat transfer rates is required to determine various transport phenomena such as water and species transport, reaction kinetics, and rate of phase change. Thermal transport also impacts design, efficiency, reliability and durability of the system [6–8].

A key thermo-physical property for thermal analysis of fuel cells is the thermal conductivity of the membrane-electrode assembly components, particularly the gas diffusion layer (GDL) [9,10]. The fibrous anisotropic micro-structure of a GDL combined with the large differences between the thermal conductivity of the solid (carbon fibers) and fluid (air/water) phases make it challenging to determine the dependence of the effective thermal conductivity on direction.

The majority of the thermal analyses of fuel cells have relied on a simplified model representation that assumes an isotropic thermal conductivity [10–12] that is determined as a combination of the parallel and series models and/or based on the geometric mean of the thermal conductivities of solid and fluid phases [11,12]. Although the thermal resistance of GDLs for the in-plane direction is higher compared to the through-plane direction, heat transfer to the bipolar plate (BPP) occurs in both directions due to the alternating nature of the land and channel areas [13]. In the few modeling studies that have considered anisotropy, parametric investigations have shown that the prescription of anisotropic properties has a major impact on current density distribution and on the relative importance of limiting transport processes [13–15]. The determination of the in-plane thermal conductivity is therefore an important parameter for thermal analysis and management of PEM fuel cells and stacks.

Theoretical prediction of the in-plane thermal conductivity of GDLs includes the work of Zamel et al. [16] who developed a numerical model to estimate the through-plane and in-plane effective thermal conductivities of a dry untreated carbon paper GDL. They studied the effects of porosity, fiber distribution and compression on the effective thermal conductivity and concluded that the impact of fiber distribution is more pronounced for the through-plane direction than the in-plane direction. The numerical results indicate that porosity is an essential determinant of the effective thermal conductivity of a GDL but not compression. Based on the results, Zamel et al. [16] proposed correlations for the effective thermal conductivity of a dry GDL with no binder or hydrophobic treatment.

GDLs are generally treated with polytetrafluoroethylene (PTFE) to render them hydophobic and enhance liquid water transport [17]. The effect of PTFE treatment on the thermal transport param-

* Corresponding author at: Department Mechanical Engineering, and Institute for Integrated Energy Systems, University of Victoria, P.O. Box 3055, Victoria, BC, V8W 3P6, Canada. Tel.: +1 7787828587; fax: +1 2507216051.
E-mail address: ehsans@uvic.ca (E. Sadeghi).

0378-7753/$ – see front matter © 2010 Elsevier B.V. All rights reserved.
doi:10.1016/j.jpowsour.2010.11.151

Nomenclature

A	cross-sectional area of fluxmeters, heat radiation area (m^2)
A_f	cross-sectional area of a fiber (m^2)
A_{in}	cross-sectional area of GDL (m^2)
a	radius of contact area between fibers (m)
b	radius of the area covered by PTFE at contact points (m)
e	emissivity, Eq. (1)
F_{ij}	view factor, Eq. (1)
k	thermal conductivity ($W\,m^{-1}\,K^{-1}$)
k_{cell}	in-plane effective thermal conductivity of each cell, Fig. 3 ($W\,m^{-1}\,K^{-1}$)
$k_{eff,in}$	in-plane effective thermal conductivity of GDL ($W\,m^{-1}\,K^{-1}$)
$k_{eff,in,o}$	in-plane effective thermal conductivity of GDL, no PTFE ($W\,m^{-1}\,K^{-1}$)
$k_{parallel}$	effective thermal conductivity based on the Parallel model ($W\,m^{-1}\,K^{-1}$)
k_{PTFE}	thermal conductivity of PTFE ($W\,m^{-1}\,K^{-1}$)
k_s	thermal conductivity of carbon fiber ($W\,m^{-1}\,K^{-1}$)
L	length of GDL sample, distance between sample holders, Figs. 1 and 3 (m)
m	number of cells
N	total number of GDL samples in the experiment
n	number of fibers in each cell
Q	heat transfer rate (W)
Q_{ij}	Radiation heat transfer between bodies i and j (W)
q	heat flux ($W\,m^{-2}$)
R_{cell}	cell thermal resistance ($K\,W^{-1}$)
R_{end}	thermal resistance at sample ends ($K\,W^{-1}$)
R_{fl}	thermal resistance of fluxmeter ($K\,W^{-1}$)
R_{GDL}	GDL thermal resistance ($K\,W^{-1}$)
R_{gr}	groove thermal resistance ($K\,W^{-1}$)
R_{junc}	total thermal resistance at each cell interface ($K\,W^{-1}$)
R_{layer}	summation of GDL and groove thermal resistance ($K\,W^{-1}$)
R_{PTFE}	thermal resistance of PTFE in contact regions of fibers ($K\,W^{-1}$)
R_{SH}	sample holder thermal resistance ($K\,W^{-1}$)
R_{tot}	total thermal resistance ($K\,W^{-1}$)
R_w	thermal resistance of wooden block ($K\,W^{-1}$)
r	fibers' mean radius (m)
T	temperature (K)
TCR	thermal contact resistance between fibers ($K\,W^{-1}$)
t	sample thickness (m)
$\bar{V}$	average volume of a fiber (m^3)
V_s	total volume of fibers (m^3)
V_{tot}	total volume of GDL sample (m^3)
W	width (m)
z	heat flow direction (m)

Greek symbols

α	radius of contact area between fibers over fiber radius, ar^{-1}
β	radius of area covered by PTFE over fiber radius, br^{-1}
λ	weight fraction of PTFE content
σ	Stefan-Boltzmann constant
ε_0	GDL porosity before PTFE treatment
θ	angle between fiber and heat flux directions
θ_m	maximum fiber angle
ϕ_s	fiber volume fraction
ℓ	fiber average length (m)

Subscripts

1	right side of the experiment setup
2	left side of the experiment setup
i	body i
j	body j
low	lower fluxmeter
r	radiation
up	upper fluxmeter

eters has been investigated by Khandelwal and Mench [18]. Their measurements for SIGRACET® GDLs showed that for 20% PTFE content, the through-plane thermal conductivity was reduced by 54% compared to untreated GDL samples; the thermal contact resistance on the other hand was not significantly affected by the variation of PTFE content. These results are opposite to expected trends from physical considerations; additional PTFE is for instance expected to displace lower conductivity air, and hence results in higher effective thermal conductivity. Karimi et al. [19] investigated the effect of PTFE coating on the through-plane conductivity and thermal contact resistance of SpectraCarb GDLs, and reported that the effective thermal conductivity of PTFE-treated GDLs increased slightly at low compression loads and decreased slightly at higher loads. For low compression loads, they also reported significantly higher thermal contact resistance values for PTFE-treated samples compared to untreated ones. This difference decreased with an increase in applied pressure.

Several experimental approaches have been proposed to measure *electrical* conductivity of GDLs. Ismail et al. [20] measured the in-plane and through-plane electrical conductivities of SIGRACET® GDLs, and found the in-plane electrical conductivity remains approximately constant with an increase in PTFE content. They also reported that the through-plane electrical contact resistance increases with PTFE content.

The micron scale of the fibers combined with the brittle nature of the GDL structure make it challenging to measure the *in-plane thermal conductivity* of such random micro-structures, and to the authors' knowledge, no experimental data has been reported in the open literature.

This paper presents a combined experimental and theoretical investigation focusing on the determination of the in-plane thermal conductivity of PTFE-coated GDLs. Building on our previous study that dealt with the through-plane conductivity and contact resistance [21], the existing test bed was modified and an experimental technique was developed that enables the measurement of in-plane thermal conductivity of fibrous porous media and thin films. Toray carbon papers TGP-H-120 with different PTFE contents are used in the experiments. The in-plane effective thermal conductivity and contact resistance are deduced from the total thermal resistance measurements by performing a series of experiments with GDL samples of different lengths but similar micro-structures. Furthermore, a compact analytical model is proposed to predict the in-plane thermal conductivity of GDLs as a function of porosity and PTFE content.

2. Experimental study

The experimental apparatus and a schematic of the test setup for the in-plane thermal conductivity measurement are shown in Fig. 1. The test chamber consists of a stainless steel base plate and a bell jar enclosing the test column. The test column consists of,

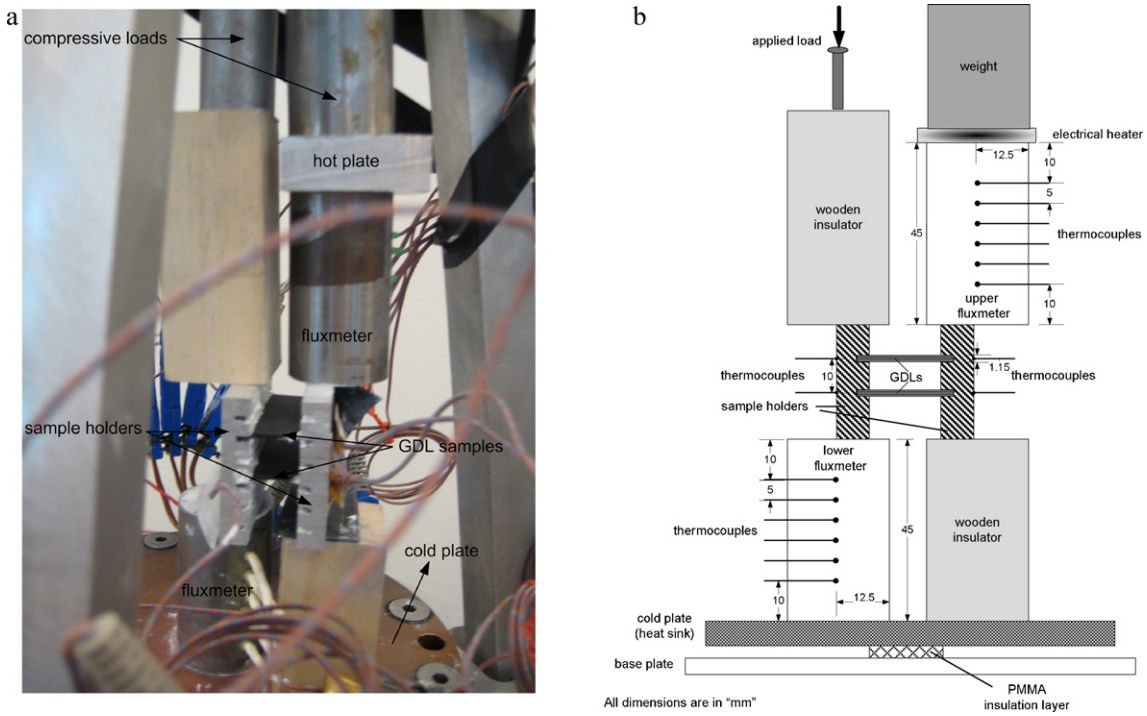

Fig. 1. (a) Experimental apparatus used for in-plane thermal conductivity measurement and (b) schematic view of the test column.

from top to bottom: the loading mechanism; the heater block; the upper fluxmeter; the upper wooden block; the sample holders; the samples; the lower fluxmeter; the lower wooden block; the heat sink (cold plate); and the polymethyl-methacrylate (PMMA) layer.

The heater block was made of aluminum in which a pencil-type electrical heater was installed. The designed cold plate consisted of a hollow copper cylinder, 1.9 cm high and 15 cm diameter. Cooling was accomplished using a closed loop water-glycol bath in which the coolant temperature can be set. The cold plate was connected to the chiller unit which adjusts the cold water temperature. A load was applied on the upper wooden block and fluxmeter to improve the contact between the sample holders and the fluxmeters.

The fluxmeters were made of standard electrolyte iron. To measure temperatures along the fluxmeters, six T-type thermocouples were attached to each fluxmeter at specific locations shown in Fig. 1(b). The thermal conductivity of the fluxmeters was known and used to measure the heat flow rate. The sample holders were made of aluminum and have two grooves with the width of 1.15 mm. Two T-type thermocouples were attached to each sample holder near the grooves to measure the temperature.

2.1. Sample preparation

Toray carbon papers TGP-H-120 with the base porosity (porosity of the untreated GDL) of 78% and a wide range of PTFE content, from 5% to 30%, were used. The thickness of GDL samples was measured using a Mitutoyo digital micrometer with the accuracy of 0.001 mm. The measurements were performed 10 times for each sample at different locations, and the average values are reported in Table 1. Rectangular test samples were cut with a width of 35 mm and different lengths.

Table 1
Thickness of examined Toray carbon papers TGP-H-120.

PTFE (%)	5	10	20	30
t (mm)	0.374	0.376	0.362	0.354

2.2. Test procedure

The experiments were performed under a vacuum to ensure negligible convection heat transfer. Depending on the thickness, a number of similar GDL samples, e.g., three sheets for TGP-H-120, were stacked together and inserted in each groove of the sample holders as shown in Fig. 1. The use of several layers of GDLs mitigated some of the experimental challenges and uncertainties: use of a single GDL layer between the sample holders leads to an excessive temperature drop across the sample holders, which in turn tremendously increases the temperatures along the upper fluxmeter, even for a small heat flux, and may burn the thermocouples. This is due to micron size cross-sectional area of the GDL. After investigating and trying different methods, the present sample holders featuring multiple grooves that can hold several GDLs was devised to overcome these challenges.

To reduce the contact resistance between the groove walls and the samples, a thin layer of thermal paste was applied inside each groove. To improve the stability of the sample holders and provide a good contact with the fluxmeters, compressive loads were applied to the upper wooden block and the upper fluxmeter; this is solely to keep the test column together. Thermal paste was also used to reduce the thermal contact resistance at the interfaces between the sample holders and the fluxmeters.

Temperatures were monitored continuously and recorded when steady-state conditions were achieved. This took approximately 7 h for each experiment. The fairly long equilibration time is due to the restricted cross sectional area through which heat transfer takes place. The temperature gradient between the hot and cold plates results in one-dimensional heat conduction from the top to the bottom of the test column. The thermal resistance network corresponding to the experimental setup is shown in Fig. 2(a). Natural convection heat losses are negligible in the vacuum chamber. Radiation heat losses from the fluxmeters and end plates can be estimated from the following relationship [22].

$$Q_{ij} = \frac{\sigma(T_i^4 - T_j^4)}{(1 - e_i/e_i A_i) + (1/A_i F_{ij}) + (1 - e_j/e_j A_j)} \quad (1)$$

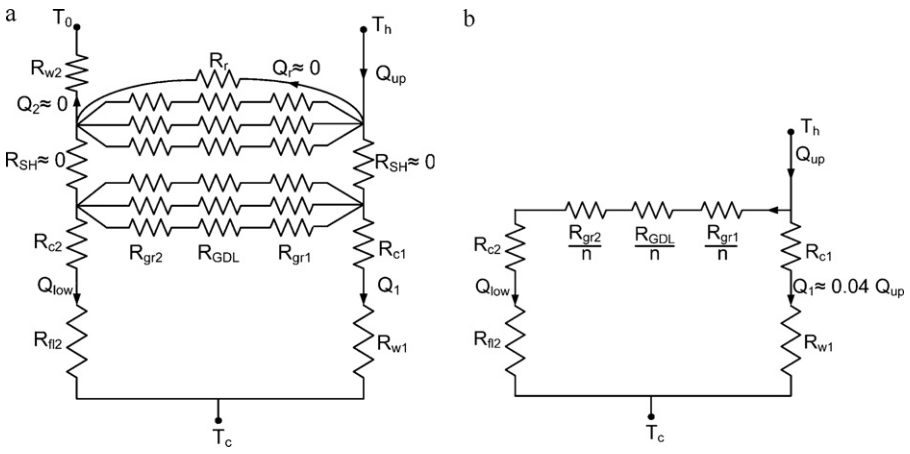

Fig. 2. (a) Complete and (b) reduced resistance network associated with the experiments.

where $\sigma = 5.67 \times 10^{-8}\,\mathrm{W\,m^{-2}\,K^{-4}}$ is the Stefan-Boltzmann constant. Q_{ij} is the radiation exchange between bodies i and j, and e is the emissivity. Also, F_{ij} is the view factor defined as the fraction of the radiation that leaves A_i and is intercepted by A_j. To find the radiation heat losses, Eq. (1) is employed which provides the maximum radiative heat transfer between two bodies. The investigated radiation losses from the fluxmeters to the wooden blocks and the chamber wall are less than 1% of the total heat flow passing the fluxmeters. Also, small temperature difference between the fibers in GDLs as well as relatively low temperature levels (less than 370 K) inside the medium ensure negligible radiation heat transfer in the GDL. Thus, heat transfer is only due to conduction and can be determined using Fourier's equation.

$$Q = -kA\frac{dT}{dz} \tag{2}$$

where dT/dz is the temperature gradient along the test column, k is the thermal conductivity of the fluxmeters, and A is the cross-sectional area of the fluxmeters. Considering negligible heat losses, the resistance network shown in Fig. 2(a) can be reduced to Fig. 2(b). The total thermal resistance between two sample holders, R_{tot}, includes the samples' thermal resistance and the resistances at the sample ends (a combination of the thermal contact resistance between the grooves and the samples and other possible resistances caused by the edges of the grooves at each end), and can be expressed as:

$$R_{\mathrm{tot}} = \frac{R_{\mathrm{layer}}}{N} = \frac{R_{\mathrm{GDL}} + R_{\mathrm{gr1}} + R_{\mathrm{gr2}}}{N} = \frac{R_{\mathrm{GDL}}}{N} + \frac{R_{\mathrm{end}}}{N} = \frac{\Delta T}{Q} \tag{3}$$

where ΔT is the temperature difference between the two sample holders and N is the total number of GDL layers stacked in the grooves. R_{GDL} and R_{end} are the thermal resistance of each sample and the total thermal resistance at the end points of each sample, respectively. There is a small difference between the heat flow values measured for the upper and lower fluxmeters due to heat losses to the lower wooden block and to experimental uncertainties; heat losses to the wooden block are about 4% of the heat flow passing the upper fluxmeter. Therefore, the actual heat flux which passes through the GDL samples is the heat flux measured at the lower fluxmeter. To ensure accuracy, this heat flow rate was used in the analysis, i.e., Eq. (3). To find the in-plane thermal conductivity, two sets of experiments were performed with different sample lengths. Under the same experimental conditions, R_{end} for both experiments was assumed to be equal. Applying Eq. (3) to both of the measurements and subtracting them, one can find the in-plane effective thermal conductivity.

$$k_{\mathrm{eff,in}} = \frac{L_1}{R_{\mathrm{GDL1}}A} = \frac{L_2}{R_{\mathrm{GDL1}}A} \tag{4}$$

$$k_{\mathrm{eff,in}} = \frac{N(L_1 - L_2)}{(R_{\mathrm{tot1}} - R_{\mathrm{tot2}})A_{\mathrm{in}}} \tag{5}$$

where L_1 and L_2 are the sample length, the distance between the two sample holders, in experiment 1 and 2, and A_{in} is the in-plane cross-section of each sample.

2.3. Uncertainty analysis

Considering the relationship for evaluating the in-plane effective thermal conductivity, i.e., Eqs. (3) and (5), the relevant parameters in the analysis can be expressed as:

$$k_{\mathrm{eff,in}} = f(Q, \Delta T, t, W, L) \tag{6}$$

The main uncertainty in our experiments is due to errors in determining the heat flux through the sample holders which leads to a maximum error of 3.7%. The maximum uncertainties for the thermocouples and the data acquisition readings are ±1 °C which introduces a maximum error of 1.8% between two sample holders. Other uncertainties including those associated with the width, thickness, and length measurements are 0.3%, 0.3%, and 0.9%, respectively. The maximum uncertainty for the thermal resistance measurements can be calculated from [23]:

$$\frac{\delta k_{\mathrm{eff,in}}}{k_{\mathrm{eff,in}}} = \sqrt{\left(\frac{\delta Q}{Q}\right)^2 + \left(\frac{\delta \Delta T}{\Delta T}\right)^2 + \left(\frac{\delta t}{t}\right)^2 + \left(\frac{\delta W}{W}\right)^2 + \left(\frac{\delta L}{L}\right)^2} \tag{7}$$

For the present study, the maximum uncertainty is estimated to be ±4.2%.

3. Analytical study

The complex micro-structure and associated heat transfer mechanism of fibrous GDLs make it difficult to develop an analytic model for the effective thermal conductivity. To model the in-plane effective thermal conductivity, a random micro-structure divided into m equally-sized cells is considered. Each cell consists of n fibers with an average radius of r and an average length of ℓ which are randomly oriented in the xy plane with an angle θ to the in-plane heat flow direction and stacked vertically in z direction, as shown in Fig. 3. The fiber angle θ can vary in this representation.

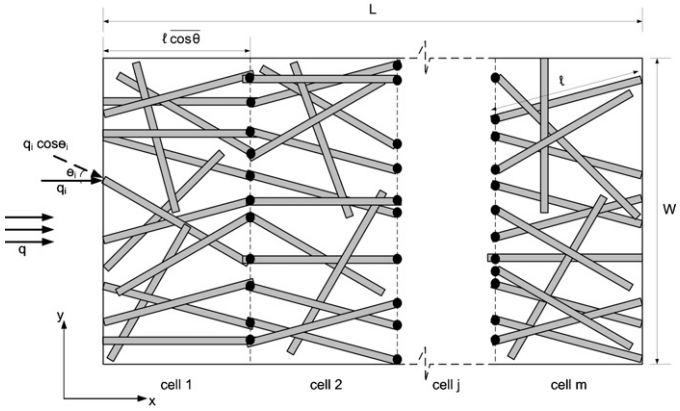

Fig. 3. Constructed micro-structure for in-plane thermal conductivity modeling.

Considering that the primary path for the heat conduction is through the fibers and heat transfer between the fibers in a cell is negligible due to large contact resistances, a parallel equivalent circuit model can be used to determine the thermal conductivity in each cell. The heat conducted through the ith fiber with an angle θ_i to the heat flux vector $\vec{q}_i$ is $q_i \cos\theta$, therefore, each fiber deviates from the parallel model by $\cos\theta_i$. Thus, the effective conductivity for each cell, k_{cell}, can be written as:

$$k_{\text{cell}} = \frac{\sum_{i=1}^{n} \cos\theta}{n} k_{\text{parallel}} = \frac{\sum_{i=1}^{n} (k_s A_f \cos\theta_i)}{(nA_f/\phi_s)} = \overline{\cos\theta}\phi_s k_s \tag{8}$$

where $\overline{\cos\theta}$ is the average of $\cos\theta_i$ in a cell. k_s and A_f is are the fiber thermal conductivity and cross-sectional area, respectively. ϕ_s is the fiber volume fraction, i.e., $\phi_s = 1 - \varepsilon_0$, where ε_0 is the GDL porosity before PTFE treatment. We assume that the heat flow is transferred from cell to cell through the junctions. The length of each cell is defined as the average conduction path in a cell, $\ell\overline{\cos\theta}$. Since the fibers are stacked together in a packed micro-structure, it is assumed that each fiber of two neighboring cells is in contact with two fibers from the top and the bottom and carries heat from them as shown in Fig. 4. The contact between the fibers at a junction is shown in Fig. 5.

To estimate the in-plane effective thermal conductivity of the medium, the total resistance is needed which can be found using the thermal resistance network shown in Fig. 6.

The number of cells as well as the number of fibers in each cell is required to evaluate the thermal resistances. These values can be found through:

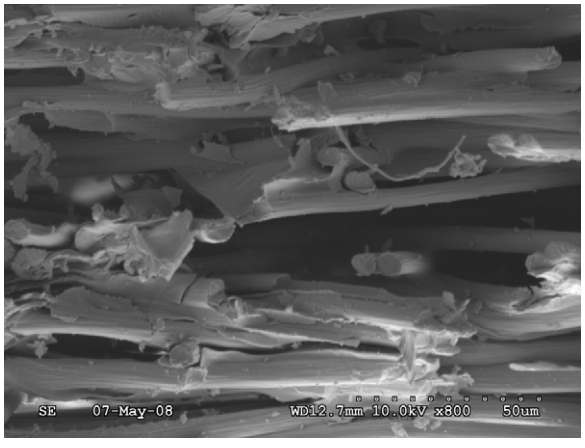

Fig. 4. In-plane SEM image of a Toray carbon paper, ×800 magnification.

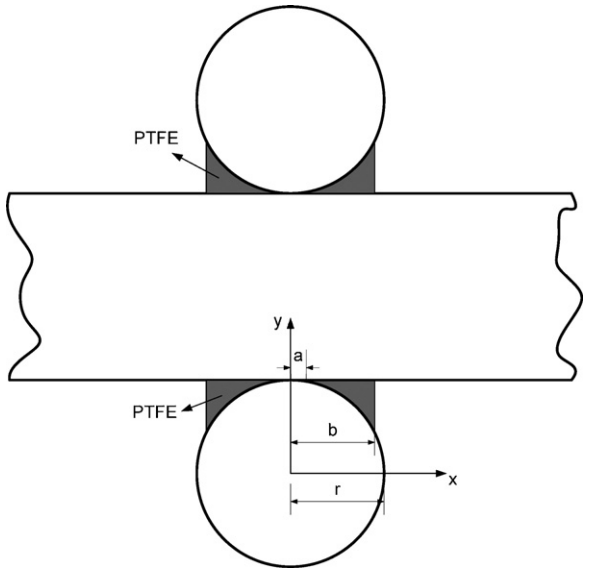

Fig. 5. Contact between fibers at a junction.

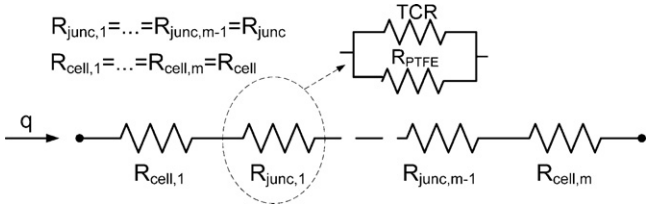

Fig. 6. Thermal resistance network of the GDL for in-plane direction.

$$m = \frac{L}{\ell\overline{\cos\theta}} \tag{9}$$

$$n = \frac{V_s}{m\bar{V}} = \frac{\phi_s V_{\text{tot}}}{m\bar{V}} = \frac{Wt\phi_s\overline{\cos\theta}}{\pi r^2} \tag{10}$$

where $\bar{V}$, W and t are the average volume of each fiber, the width and the thickness of the GDL sample. The contact resistance between two fibers can be expressed as the summation of constriction and spreading resistances [24].

$$\text{TCR} = \frac{1}{2k_s a} = \frac{1}{2k_s r\alpha} \tag{11}$$

where a is the radius of contact area between fibers and α is a/r. A portion of PTFE in GDLs covers the contacting fibers providing an additional path for the heat flow from one fiber to another. The thermal resistance of this path based on the geometry shown in Fig. 5 can be expressed as:

$$\frac{1}{R_{\text{PTFE}}} = \frac{1}{2}\int \frac{1}{dR} = \frac{1}{2}\int_a^b \frac{k_{\text{PTFE}}(2\pi x\, dx)}{(r-y)} \tag{12}$$

$$R_{\text{PTFE}} = \frac{1}{\pi k_{\text{PTFE}} r}\left(\int_\alpha^\beta \frac{u\, du}{1-\sqrt{1-u^2}}\right)^{-1} \tag{13}$$

where $\beta = b/r$ and b is the radius of the area covered by PTFE around the contacting fibers, see Fig. 5. The total thermal resistance at each cell interface R_{junc} can be expressed as a parallel combination of the thermal resistances of $2n$ contact regions.

$$R_{\text{junc}} = \frac{(TCR^{-1} + R_{\text{PTFE}}^{-1})^{-1}}{2n} \tag{14}$$

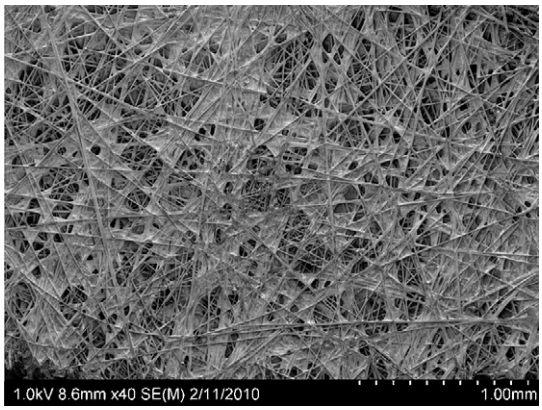

Fig. 7. SEM image of Toray carbon paper TGP-H-120 with 5% PTFE treatment, ×40 magnification.

Referring to Fig. 6, the total resistance can be written as:

$$R_{tot} = mR_{cell} + (m-1)R_{junc} \tag{15}$$

where R_{cell} is the cell thermal resistance which can be found using Eq. (8).

$$R_{cell} = \frac{\ell}{\phi_s k_s W t} \tag{16}$$

Finding the total thermal resistance from Eq. (15), one can evaluate the effective thermal conductivity using the following relation.

$$k_{eff,in} = \frac{L}{R_{tot} W t} \tag{17}$$

For the sample with no PTFE coating, Eq. (17) can be simplified to:

$$k_{eff,in,0} = \frac{4\alpha L \phi_s k_s \overline{\cos\theta}}{4\alpha L + \pi(m-1)r} \cong \frac{4\alpha \ell \phi_s k_s \overline{\cos\theta}^2}{4\alpha \ell \overline{\cos\theta} + \pi r} \tag{18}$$

Based on scanning electron microscopy (SEM) images of Toray carbon papers, Fig. 7, the fiber angle with respect to the heat flow direction, θ, can vary arbitrarily between $-\theta_m$ and θ_m, where $0 \le \theta_m \le 90$. Considering an arbitrary distribution of fiber angle without preferential direction, $\overline{\cos\theta}$ can be estimated through:

$$\overline{\cos\theta} = \frac{\sum_{i=1}^{n} \cos\theta_i}{n} = \frac{\sum_{i=1}^{n} \cos\theta_i \Delta\theta}{n\Delta\theta} = \frac{\sum_{i=1}^{n} \cos\theta_i \Delta\theta}{2\theta_m} \tag{19}$$

where $\Delta\theta = [\theta_m - (-\theta_m)]/n$. The number of fibers in a cell is large enough, $n \cong 35{,}000$, to convert the series in Eq. (19) to an integral.

$$\overline{\cos\theta} = \frac{\sum_{i=1}^{n} \cos\theta_i \Delta\theta}{2\theta_m} = \frac{\int_{-\theta_m}^{\theta_m} \cos\theta d\theta}{2\theta_m} = \frac{\sin\theta_m}{\theta_m} \tag{20}$$

We measured the fiber angle in the SEM image, Fig. 7, and our analysis shows that the majority of fiber angles are between −75 and 75, i.e., $\theta_m = 75$. Other specifications of the Toray carbon paper required for the present model are listed in Table 2.

Table 2
Input data for the in-plane thermal conductivity modeling of Toray carbon papers.

r (μm)	ℓ (μm)	k_s (W m^{-1} K^{-1})	k_{PTFE} (W m^{-1} K^{-1})
4.25	325 [25]	120 [26]	0.649 [27]

Toray carbon papers have the highest through-plane thermal conductivity among different available carbon papers with similar porosity due to the contribution of the binder to heat transfer in the carbon paper GDL [16]. The binder fills the gaps between fibers and provides a better contact. The thermal conductivity of the binder can be assumed to be equal to that of the carbon fibers [16]. The actual amount of binders at contact points and as a result the contact area between contacting fibers are unknown. To determine the in-plane thermal conductivity, the value for α was estimated as 0.1 based on SEM observation shown in Fig. 4.

The PTFE conductivity is very low compared to the thermal conductivity of carbon fibers and its effect on the in-plane thermal conductivity is small as shown later. However, to include the effect of PTFE variation in the model, we assume that the radius ratio of PTFE to carbon fiber, β, is 0.25 for 5% and 1 for 30% PTFE content, and remains constant at 1 for higher values of PTFE content. The following relationship is developed for the PTFE content at the contact points of fibers.

$$\beta = 0.25 + 3(\lambda - 0.05) \tag{21}$$

where λ is the weight fraction of PTFE, $0.05 \le \lambda \le 0.3$ This is an approximate relationship, which is proposed based on SEM images of carbon papers with different PTFE contents. However, due to the very low thermal conductivity of PTFE, variants of this distribution do not have a significant impact on the model predictions.

4. Results and discussion

Measurements were taken for TGP-H-120 samples with different PTFE contents. A summary of the experimental results is shown in Table 3. The measurements were performed at an average sample temperature of 65–70 °C. There is a small difference between the measured values of heat fluxes in the upper and the lower fluxmeters due to heat losses and experimental uncertainties. Due to heat losses to the lower wooden block, the readings from the lower heat flux were used for thermal resistance calculations. As shown in Table 3, the in-plane thermal conductivity appears to increase slightly with PTFE content as a result of reduced contact resistance between fibers. However, this variation is within the uncertainty band of the present experimental measurement. The thermal conductivity values obtained lie between the values predicted by Zamel et al. [16] and those of the manufacturer [28]. Zamel et al. [16] reported an in-plane thermal conductivity value of 10 W m^{-1} k^{-1} based on numerical simulations at a temperature of 68 °C; the value reported in the manufacturer's data sheet [28] is 21 and 23 W m^{-1} k^{-1} at the room temperature and 100 °C, respectively.

Table 3
Summary of experimental results for Toray carbon paper TGP-H-120 with different PTFE contents.

PTFE content (%)	L (mm)	Q_{up} (W)	Q_{low} (W)	R_{layer} (K W^{-1})	R_{end} (K W^{-1})	$K_{eff,in}$ (W m^{-1} W^{-1})
5	11.02	5.72	5.29	63.21	14.27	17.39
	14.34	5.49	5.17	77.79		
10	11.20	5.61	5.35	65.33	15.42	17.33
	14.29	5.53	5.14	78.88		
20	11.37	5.73	5.41	67.13	17.19	17.58
	14.55	5.46	5.25	81.41		
30	11.28	5.77	5.34	66.95	18.05	17.81
	14.67	5.62	5.20	82.31		

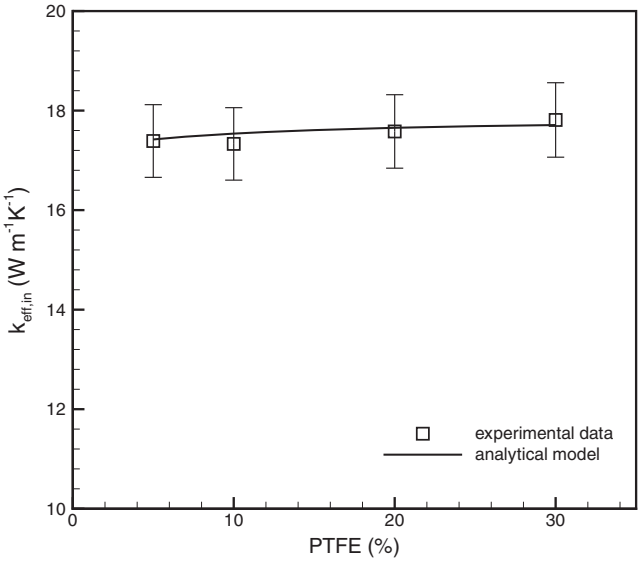

Fig. 8. Comparison of the present experimental data and analytical model for in-plane thermal conductivity of Toray carbon paper TGP-H-120 over a range of PTFE content.

By increasing PTFE content, the number of PTFE coated fibers in contact with the grooves increases. This results in a higher contact resistance between the GDL samples and the groove walls. This resistance R_{end} increases 26% by increasing PTFE content from 5% to 30% as shown in Table 3.

The developed analytical model for the in-plane effective thermal conductivity is compared with the experimental data in Fig. 8. Good agreement is obtained with a maximum deviation of 5%. We note that the model reproduces the slight increase in effective thermal conductivity with PTFE content observed in the experimental data.

In practice, due to the electrochemical reaction, overall water transport and phase change, water in both vapor and liquid form is present in a fuel cell [2]. This water may impact the thermal conductivity while passing through the GDL. The thermal conductivity of humidified gasses or water is several orders of magnitude lower than the thermal conductivity of carbon fibers, and considering the relatively parallel paths for the heat transfer through them, the effect of water content on the in-plane thermal conductivity of GDLs is expected to be minimal when the GDL is not significantly flooded. In the through-plane direction, the effect of water is likely much more important as it can provide additional pathways for heat transfer in the contact regions between fibers. Burheim et al. [29] compared the through-plane thermal conductivity of dry and humidified GDLs and showed that the conductivity increases by about 70% for low contact pressures when water was added to the GDL. This issue needs to be further investigated.

5. Summary and conclusions

A new thermal measurement technique was developed to measure the in-plane thermal conductivity of GDLs for various PTFE contents. Toray carbon papers TGP-H-120 with PTFE content of 5–30% were used in the experiments. The experiments were complemented by a compact model for the in-plane thermal conductivity that accounts for heat conduction through randomly oriented fibers, contact area between fibers, and PTFE covered regions. The model predictions are in good agreement with experimental data over a range of PTFE content.

An important finding is that the in-plane effective thermal conductivity remains almost unchanged, $k \approx 17.5\,\mathrm{W\,m^{-1}\,K^{-1}}$, over a wide range of PTFE content; this value is approximately 12 times higher than the through-plane conductivity. However, the thermal contact resistance and the end effects increase with the PTFE content due to increased number of PTFE coated fibers.

In addition to providing for the first time through-plane effective conductivity data, this work clarifies the effect of PTFE content on the effective thermal conductivity and contact resistance of GDLs, and provides input data for fuel cell models.

Acknowledgements

The authors are grateful for the financial support of the Natural Sciences and Engineering Research Council (NSERC) of Canada, and the Canada Research Chairs Program.

References

[1] N. Djilali, D. Lu, Int. J. Therm. Sci. 41 (2002) 29–40.
[2] T. Berning, N. Djilali, J. Electrochem. Soc. 150 (2003) A1589–A1598.
[3] G. Maggio, V. Recupero, C. Mantegazza, J. Power Sources 62 (1996) 167–174.
[4] S. He, M.M. Mench, S. Tadigadapa, Sens. Actuators A: Phys. 125 (2006) 170–177.
[5] P.J.S. Vie, S. Kjelstrup, Electrochim. Acta 49 (2004) 1069–1077.
[6] A. Kusoglu, Y. Tang, M.H. Santare, A.M. Karlsson, S. Cleghorn, W.B. Johnson, J. Fuel Cell Sci. Technol. 6 (2009) 011012–011019.
[7] D.P. Wilkinson, H.H. Voss, K. Prater, J. Power Sources 49 (1994) 117–127.
[8] P. Rama, R. Chen, J. Andrews, J. Power Energy 222 (2008) 421–441.
[9] A. Hakenjos, H. Muenter, U. Wittstadt, C. Hebling, J. Power Sources 131 (2004) 213–216.
[10] H. Ju, H. Meng, C.Y. Wang, Int. J. Heat Mass Trans. 48 (2005) 1303–1315.
[11] J.J. Baschuk, X. Li, J. Power Sources 142 (2005) 134–153.
[12] J.J. Hwang, J. Electrochem. Soc. 153 (2006) A216–A224.
[13] P.C. Sui, N. Djilali, J. Power Sources 161 (2006) 294–300.
[14] J.G. Pharoah, K. Karan, W. Sun, J. Power Sources 161 (2006) 214–224.
[15] C.J. Bapat, S.T. Thynell, J. Power Sources 179 (2008) 240–251.
[16] N. Zamel, X. Li, J. Shen, J. Becker, A. Wiegmann, Chem. Eng. Sci. 65 (2010) 3994–4006.
[17] G.G. Park, Y.J. Sohn, T.H. Yang, Y.G. Yoon, W.Y. Lee, C.S. Kim, J. Power Sources 131 (2004) 182–187.
[18] M. Khandelwal, M.M. Mench, J. Power Sources 161 (2006) 1106–1115.
[19] G. Karimi, X. Li, P. Teertstra, Electrochim. Acta 55 (2010) 1619–1625.
[20] M.S. Ismail, T. Damjanovic, D.B. Ingham, M. Pourkashanian, A. Westwood, J. Power Sources 195 (2010) 2700–2708.
[21] E. Sadeghi, N. Djilali, M. Bahrami, J. Power Sources 196 (2011) 246–254.
[22] F.P. Incropera, D.P. DeWitt, Fundamentals of Heat and Mass Transfer, fourth ed., John Willey and Sons, New York, USA, 1996 (Chapter 13).
[23] J.R. Taylor, An Introduction to Error Analysis: The Study of Uncertainties in Physical Measurements, second ed., University Science Books, Sausalito, US, 1997 (Chapter 3).
[24] H.S. Carslaw, J.C. Jaeger, Conduction of Heat in Solids, second ed., Oxford Press, London, 1959.
[25] N. Parikh, J. Allen, R.S. Yassar, J. Power Sources 193 (2009) 766–768.
[26] J. Ramousse, S. Didierjean, P. Lottin, D. Maillet, Int. J. Therm. Sci. 47 (2008) 1–6.
[27] Web: http://www.boedeker.com/ptfe_p.htm.
[28] Web: http://www.fuelcell.com/techsheets/TORAY-TGP-H.pdf.
[29] O. Burheim, P.J.S. Vie, J.G. Pharoah, S. Kjelstrup, J. Power Sources 195 (2010) 249–256.